12 Mar 1991, 10:30 am - 12:00 pm

Soils Parameters and Constitutive Relations Under Multiaxial Cyclic Loading

M. Reza Salami

North Carolina Agricultural and Technical State University, Greensboro, North Carolina

Proceedings: Second International Conference on Recent Advances in Geotechnical Earthquake Engineering and Soil Dynamics, March 11-15, 1991 St. Louis, Missouri, Paper No. 1.11

Soils Parameters and Constitutive Relations Under Multiaxial Cyclic Loading

M. Reza Salami
Assistant Professor, North Carolina Agricultural and Technical State University, Greensboro, North Carolina

SYNOPSIA: A generalized constitutive model based on the theory of plasticity is proposed and utilized to characterize stress-deformation behavior of soils and geological materials under complex and cyclic multiaxial loadings. It allows for factors such as hardenings, volume changes, stress paths, cohesive and tensile strengths and variation of yield behavior with mean pressure. It is applied to characterize behavior of soils, concrete and rocks. The Constants for the model are determined from series of available laboratory tests conducted under different initial confinements, cyclic hydrostatic preloading and stress paths obtained by using multiaxial and cylindrical triaxial testing devices. The model is verified with respect to observed laboratory responses. Overall, the proposed model is found suitable to characterize the behavior of geological materials such as soils, concrete and rocks and involves less or equal number of constants compared to available models of similar capabilities and is easier to implement in numerical solution procedures.

INTRODUCTION

Characterization of stress-deformation behavior of concrete has been a subject of active research for a long time. Linear elastic, nonlinear (piecewise linear) elastic, elastic-plastic and endochronic models have been proposed and used by various investigators and the literature on the subject is very wide An excellent review of various models together with their implementation in numerical (finite element) procedures is presented by the subcommittee on the subject chaired by Chen et al. (1980) and Task Committee (1982). ; a review of this paper is present a general model to characterize ultimate (and failure) and hardening (softening) response in the context of the theory of plasticity.

PROPOSED MODEL

A general expression for hardening (or softening) yield function F can be expressed by Salami (1986,1987) and Desai et al. (1984,1983a,1983b,1982,1974) as

$$F = F\,(J_i,\ I_i^p,\ K_j,\ a_m) \tag{1}$$

where J_i (i = 1,2,3) = invariants of the stress tensor, I_i^p (i = 1,2,3) = invariants of the plastic strain tensor, K_j = joint or mixed invariants, $K_1 = \sigma_{ij}\,\varepsilon_{ij}^p$, $K_2 = \sigma_{ij}\,\sigma_{jk}\,\varepsilon_{ij}^p$, $K_3 = \sigma_{ij}\,\varepsilon_{ik}^p\,\varepsilon_{ki}^p$ and $K_4 = \sigma_{ij}\,\sigma_{jk}\,\varepsilon_{kl}^p\,\varepsilon_{li}^p$, a_m (m = 1,2,3, . . .) = scalar or tensor valued internal variables. The direct invariants J_i and I_i^p are defined as

$$J_1 = \sigma_{ii} \qquad I_1^p = \varepsilon_{ii}^p$$

$$J_2 = \frac{1}{2}\,\sigma_{ij}\,\sigma_{ji} \qquad I_2^p = \frac{1}{2}\,\varepsilon_{ij}^p\,\varepsilon_{ji}^p$$

$$J_3 = \frac{1}{3}\,\sigma_{ij}\,\sigma_{jk}\,\sigma_{ki} \qquad I_3^p = \frac{1}{3}\,\sigma_{ij}^p\,\sigma_{jk}^p\,\sigma_{ki}^p$$

The definition of J_3 used here is different from $J_3 = \sigma_1\,\sigma_2\,\sigma_3$ often used by Desai et al.(1983a,1983b) and Faruque (1980). This is because if one of the (principal) stresses is zero or near to zero, $J_3 = \sigma_1\,\sigma_2\,\sigma_3$ may cause (computational) difficulties for involving use of the third stress invariant Desai (1983a). A special case of Eq. (1) expressed as a polynomial in J_1, $J_2^{1/2}$ and $J_3^{1/3}$ for hardening and softening response has been studied previously for geological materials such as soils, Desai et al. (1983a,1983b,1982). Hence, only brief details of this development are given here with major attention to the modifications for characterizing behavior of concrete.

One of the functions used to define yield in the context of incremental plasticity for describing behavior of soils Desai et al. (1984,1983a)) is given by

$$J_{2D} + \alpha\,J_1^2 - \beta\,J_1 J_3^{1/3} - \gamma\,J_1 - k^2 = 0 \tag{2}$$

where J_{2D} = second invariant of the deviatoric stress tensor, and α, β, γ, k = response functions. For the behavior of soils, α, γ and k were associated with the ultimate surface, whereas β was adopted as growth function (hardening or softening).

Figures 1-3 show plots of F in the J_1 - $\sqrt{J_{2D}}$, triaxial and octahedral planes, respectively. The parameter k is proportional to the cohesive strength of the material and represents the values of $\sqrt{J_{2D}}$ for $J_1 = 0$, Fig. 1. For cohesionless soils k = 0 and F passes through the origin in Figs. la, lb and lc, and for many soils k can be assumed to be constant which implies a circular yield surface on the π - plane . To avoid use of variable k, the function in Eq. (2) is modified for cohesive soils. In order to include the cohesion and the tensile strength in the ultimate criterion, a translation of the principal stress space along the hydrostatic axis is performed as shown in Fig. 4. New ultimate function becomes as

$$F = J^*_{2D} + \alpha\,J^*_1{}^2 - \beta\,J^*_1 J^*_3{}^{1/3} - \gamma\,J^*_1 \tag{3}$$

For material ultimate

$$J^*_{2D} + \alpha\,J^*_1{}^2 - \beta\,J^*_1 J^*_3{}^{1/3} - \gamma\,J^*_1 = 0 \tag{4}$$

where

$$J^*_1 = \sigma^*_{11} + \sigma^*_{22} + \sigma^*_{33} \tag{5a}$$

$$J^*_{2D} = \frac{1}{6}[(\sigma^*_{11} + \sigma^*_{22})^2 + (\sigma^*_{22} + \sigma^*_{33})^2 + (\sigma^*_{11} + \sigma^*_{33})^2] + \sigma^*_{12}{}^2 + \sigma^*_{23}{}^2 + \sigma^*_{13}{}^2 \quad (5b)$$

$$J^*_3 = \frac{1}{3}\sigma^*_{ij}\sigma^*_{mn}\sigma^*_{ni} = \frac{1}{3}T_r(\sigma^*)^3 \text{ or}$$

$$J^*_3 = \frac{1}{3}(\sigma^*_{11}{}^3 + \sigma^*_{22}{}^3 + \sigma^*_{33}{}^3) \quad (5c)$$

The resulting normal ultimate stresses σ^*_{11}, σ^*_{22} and σ^*_{33} in Eqs. (5) are then expressed as

$$\sigma^*_{11} = \sigma_{11} + R \quad (6a)$$

$$\sigma^*_{22} = \sigma_{22} + R \quad (6b)$$

$$\sigma^*_{33} = \sigma_{33} + R \quad (6c)$$

and

$$R = a\,p_a \quad (7)$$

where a = dimensionless number and p_a = atmospheric pressure. For cohesionless geological materials such as soil, concrete and rocks, R = 0, and the resulting ultimate function in Eq. (3) reduces to Eq. (2). If the uniaxial tensile strength f_t is not determined experimentally, Hannant (1972), Lade (1982) and Mitchell (1976) give an approximate formula relating f_t to the unconfined compression strength f_{cu} through the following power function as unconfined compression strength through the following power function as

$$f_t = T\,p_a\left(\frac{f_{cu}}{p_a}\right)^t \quad \text{(Compression Positive)} \quad (8)$$

where T, t = dimensionless numbers, f_t = uniaxial tensile strength, f_{cu} = unconfined compression strength and p_a = atmospheric pressure.

Once f_t is known, the value of R can be estimated. From studies conducted by Lade (1982), R was found to be 0.3% to 1.4% greater than f_t. In other words,

$$1.003\,f_t \le R \le 1.014\,f_t \quad (9a)$$

or

$$1.003\,f_t \le a\,p_a \le 1.014\,f_t \quad (9b)$$

With the estimated value of "R," the resulting stresses in Eqs. (6) are calculated and then substituted into the expression for the `stress invariants given by Eqs. (5). The parameters α and γ for ultimate surface are determined by substituting ultimate stresses for various stress paths in Eqs. (6) and then substituting in Eq. (3). Hence, we get a set of simultaneous equations which can be solved.

Comments

Almost most the models involve yield or loading surfaces expressed in terms of J_1 and J_2, with the exception of the model by Lade which also involves J_3, defined by an internal variable which is often a measure of plastic strains. Most of these models involve two or more surfaces to define yield failure and fracture. The model proposed here is expressed in terms of J_1, J_2, and J_3 with hardening defined by using various measures of plastic strains. Some of the distinguishing features of the proposed model are:

(1) Figures 1-3 show that the proposed model involves only one continuous surface which describes yield or loading surfaces by a single function, which also describes the ultimate behavior; as stated earlier, the traditional failure is defined in the proposed model by one of the functions with $\beta = \beta_f \le \beta_u$.

(2) Because only one function defines the entire behavior (hardening and ultimate), the number of required parameters is smaller than the previous multi-surface models.

(3) Since intersections (singularities) of two or more surfaces are avoided, the model is easier to implement for numerical computations.

(4) The function F (Eq. 3) plots continuous and convex in the stress spaces, Figs. 1-3, for both hardening and ultimate responses of many (geological) materials. As a result, it can be implemented in the context of the classical theory of plasticity based on the stability criterion, Drucker et al. (1952) and Drucker (1951).

(5) A single definition of growth function β can simulate hardening and softening (described subsequently) and include effects of stress path, volume change and coupling of shear and volumetric responses. As a result, the model is simplified significantly.

DETAILS OF PROPOSED MODEL

The model is Eq. (3) is capable of simulating the entire hardening, ultimate, hardening and softening behavior of concrete.

Ultimate Behavior

At ultimate, Eq. (3) reduces to

$$J^*_{2D} + \alpha J^*_1{}^2 - \beta J^*_1 J^*_3{}^{1/3} - \gamma J^*_1 = 0 \quad (10)$$

Then the ultimate state can be defined by using these constants, α, γ and R. It is usually difficult to perform hydrostatic extension tests. Hence, the value of $J_1 = \delta = -3R$, $(J_1, \sqrt{J_{2D}})$ can be found by extending ultimate envelopes (for different stress paths) in the $J_1, \sqrt{J_{2D}}$ space as the intersection with the J_1 on the negative side. As an approximation, the extension can be adopted as a straight line from the intersection of the ultimate envelop with $\sqrt{J_{2D}}$-axis to the intersection with the J_1-axis. This approximation will be more reliable if test data for low values of J_1; e.g., unconfined compression tests, are available.

Since value of δ is unique, only one such envelope can be used; however, it may be appropriate to adopt an average value of d for different stress paths if they are (slightly) different.

Once 3R is found, the values of α and β are found by a least square procedure in Eq. (3) with a number of points, $(J_1, \sqrt{J_{2D}})$, at the ultimate of observed stress-strain curves for different stress paths.

Growth Function, β

The growth function to define hardening and softening is expressed as

$$\beta((\xi, r_D) = \beta_u\left[1 - \frac{\beta_a}{i + \xi^{\eta_1}\left[1 - \beta_b\,(r_D)^{\eta_2}\right]}\right] \quad (11)$$

where $\beta_u = 3\alpha$, β_a and η_1 = constants determined from hydrostatic compression test as shown in Fig. 5, β_b and η_1 = constants determined

from shear or coupled (shear and volumetric) tests as shown in Fig. 6, i = elastic limit (for material showing plastic yielding from the beginning of loading i = 0), ξ = trajectory of plastic strains

$$\xi = \int (d\varepsilon_{ij}^{p} d\varepsilon_{ij}^{p})^{1/2} \qquad (12)$$

r_D ratio of trajectory of deviatoric plastic strains $\xi_D = \int (dE_{ij}^{p} dE_{ij}^{p})^{1/2}$ to ξ and E_{ij}^{p} = deviatoric plastic strain tensor. The inclusion of r_D allows for coupling of shear and volumetric responses and stress paths and is guided by the observed plots of r_V vs r_D as shown in Fig. 7, where r_V trajectory of volumetric plastic strain $= \frac{1}{\sqrt{3}} \int (d\varepsilon_{ij}^{p} d\varepsilon_{ij}^{p})^{1/2}$ = volumetric plastic strain tensor. It can be seen that irrespective of the stress path followed, the relation between r_V and r_D can be assumed to be essentially invariant. For an isotropic material that hardens isotropically, the relation is bounded by unity. At the end of hydrostatic compression test, $1 \leftarrow r_V$ and $0 \leftarrow r_D$ and at ultimate $0 \leftarrow r_V$, and $1 \leftarrow r_D$.

A plot of the growth function β is shown in Fig. 8. For small or zero values of ξ, the value of

$\infty \leftarrow \beta$; for computational purposes a large negative value -10000 can be assumed. For continuously hardening behavior the function approaches the value of $\beta_u = 3\alpha$. The peak or failure ($\beta_p = \beta_f$) lies below β_u After peak, and during softening, the function can be defined as β_s (ξ, r_D, ξ_V/ξ_D) and can involve different values of the constants. In this paper, only the hardening and ultimate (failure) responses are considered.

β_a and η_1, Fig. 5, are found by plotting -ln (ξ_V) vs ln (1 - β/β_u) from HC tests as intercept and slope of the (average) straight line. The results from (shear) stress path tests are plotted in terms of -ln(r_D) vs

$$\ln \left[\frac{1 - \beta_a}{\xi^{\eta_1}(1 - \frac{\beta}{\beta_u})}\right].$$

The intercept and the slope of the average straight line yields values of β_b and η_2 , Fig. 6.

Elastic Constants

For elastic-plastic hardening characterization, it is necessary to find constants such as elastic modulus, E, and Poisson's ratio, ν. The value of E is found as (average) slope of the unloading-reloading portion of the stress-strain curves; often the curves for the CTC path are used for this purpose. The value of Poisson's ratio can be found from the measurements of the (principal) strains, ε_1, ε_2, ε_3.

APPLICATIONS

Behavior of silty sand is modelled and verified by using the proposed model. Comprehensive laboratory tests under various stress paths, Fig. 9, using the multiaxial testing device performed and reported by Desai et al. (1983a) and Munster (1981) are used.

Silty Soil

This soil is obtained from Urban Mass Transportation Administration test section at Pueblo, Colorado, Desai et al. (1983b). The grain size for this soil is within the range of 0.009 mm ≤ Diameter of grain ≤ 0.18. The soil is well graded and has an optimum moisture content of 9% Desai et al. (1983b) and Janardhanam (1980).

Five tests, including the Hydrostatic (HC) test, are used to obtain the material constants associated with the proposed model. Detailed of these tests are given by Desai et al. (1983b) and Janardhanam (1980).and Munster (1981) . Table 1 shows the densities and moisture contents for these tests.

TABLE 1. Densities, Moisture Contents and the Initial Confining Pressures for the Tests on the Silty Sand.

Test	Density (g/cm^3)	Moisture Content (%)	Initial Confining Pressure (psi)
HC	1.86	9	0
CTC	1.92	9	10
SS	2.07	9	20
CTE	2.02	9	20
TC	2.03	9	25

1.0 psi = 6.89 kPa 1.0 in. = 2.54 cm. 1.0 kg = 2.2 lb.

Multiaxial Testing

For multiaxial testing 4 x 4 x 4 inch (10.16 x 10.16 x 10.16 cm) cubical specimens were used. The testing program consisted of HC, CTC, SS, CTE and TC, as shown in Fig. 9, tests with initial hydrostatic pressure $\sigma_o = J_1/3$ = 10, 20, 20, 25 psi (68.9, 137.8, 137.8 , 172.25 kPa). All specimens gradually were first loaded cyclically along the hydrostatic axis (HC) up to σ_o and then subjected to deviatoric cyclic loading along CTC, SS, CTE and TC paths with increasing octahedral shear stress to failure. Four various stress paths were used for finding ultimate parameters.

Material Constants

The values of the material constants for silty sand is obtained by using the foregoing procedures. Its values are given in Table 2 .

VERIFICATION

The proposed models was verified by predicting laboratory test results under different stress paths. Here the following incremental constitutive equations were integrated along a given stress path, starting from a given initial (hydrostatic) condition:

$$\{d\sigma\} = [C^{ep}]\{d\varepsilon\} = ([C^{e}] - [C^{p}])\{d\varepsilon\} \qquad (12)$$

where $\{d\sigma\}$ and $\{d\varepsilon\}$ = vectors of incremental stresses and strain, respectively, and $[C^{ep}]$ = elastic-plastic constitutive matrix with $[C^{e}]$ = its elastic part and $[C^{p}]$ = its plastic part. The latter was derived by using the theory of plasticity, Drucker (1952), with F in Eq. (3) as the yield function with the normality rule

$$d\varepsilon_{ij} = \lambda \frac{\partial F}{\partial \sigma_{ij}} \qquad (13)$$

and the consistency condition dF = 0; here λ = scalar proportionality parameter. Note that the matrix $[C^{ep}]$ is expressed into terms of stress, stress increments and the material constants.

TABLE 2. Material Constants for Silty Sand from Different Stress Path Tests

Material Constants for silty Sand			
		English Units	SI Units
Elastic Constants	K	9791.67 psi	67.47 MPa
	G	3507.46 psi	24.17 MPa
	E	9400 psi	64.77 MPa
	ν	0.34	0.34
Constants for Ultimate Yielding	α	0.1578	0.1578
	γ	3.10 psi	21.36 kPa
	$\delta = 3R$	0.070 psi	0.48 kPa
Constants for Hardening	β_a	6.201×10^{-4}	6.201×10^{-4}
	η_1	9.985×10^{-1}	9.985×10^{-1}
	β_b	8.46×10^{-1}	8.46×10^{-1}
	η_2	7.98×10^{-1}	7.98×10^{-1}

1.0 psi = 6.89 kPa

Silty soil

The predicted responses were compared with typical observed curves. This verification included observed curves for HC, CTC, and TC paths used to find the constants, and the results of the SS and circular stress paths that were not used in the determination of constants.

Figures 1-3 show ultimate envelopes in (J_1-$\sqrt{J_{2D}}$), octahedral and triaxial planes. Figures 10-17 show comparisons between predictions and observations (silty soil) for CTC (10.0 psi), TC (10.0 psi), SS (20.0 psi), HC and circular path tests, respectively. The predictions for the volumetric response were obtained by plotting volumetric strain ε_v vs axial strain, ε_1. These results indicate that the model can predict the stress-strain and volumetric behavior satisfactorily.

In this study, unloading and reloading are assumed to be elastic and linear is defined by the elastic constant (E, ν).

CONCLUSIONS

Ultimate surface for frictional and nonfrictional such as soil, concrete and rocks materials is mostly captured by a general three-dimensional ultimate criterion formulated in terms of first and third stress invariants and second deviatoric stress invariant of the stress tensor to provide a simple and efficient way to define continuous yielding and hardening behavior. Since it involves only a single function to define both the ultimate yield and pre-ultimate yielding, it is considered to be simpler compared to the previously used two-surface models that require two separate functions. Since the function proposed is continuous, it also avoids the singularity point at the intersection of two functions in the previous models, thus reducing the difficulties associated with computer implementation. This ultimate criterion involves only three independent materials. The material constants can be determined from simple tests such as hydrostatic compression, uniaxial compression and triaxial compression or biaxial tests. For the purpose of including values of tensile strength in ultimate criterion for frictional material, it is necessary to include the uniaxial tensile strength in the parameter determination. A simple expression for evaluation of uniaxial tensile strength on the basis of the uniaxial compressive strength is given by Lade (1982).

The proposed hardening function expressed in terms of the total plastic strain and ratio of deviatoric to total plastic strain is capable of accounting for the coupling of shear and volumetric responses and for the stress dependency. Also, the proposed model provides satisfactory predictions for observed behavior under a variety of stress paths. The proposed model predictions are shown in Figs. 10 to 17 with a dashed line. The correlation between the experimental results and analytical predictions are very good and provide a simple alternative approach for developing constitutive models for engineering materials such as soils, concrete, and rocks.

ACKNOWLEDGMENT

The author would like to express his appreciation to his chairman of the Department, Professor K. H. Murray, for his reviewing of the manuscript.

REFERENCES

Chen, W. F. and Ting, E. C. (1980), "Constitutive Models for Concrete Structure,".Journal of the Engineering Mechanics Division, ASCE, Vol. 106, No. EM1, pp. 1-19.

Desai, C. S. and Faruque, M. O. (1984), "A Constitutive Model for Geological Materials, " Journal of Eng. Mech. Div., ASCE, Vol. 110, pp. 139-148

Desai, C. S. (1983a), "A General Basis for Yield, Failure and Potential Functions in Plasticity," Int. J. Num. Analyt. Methods in Geomech. Vol. 4, pp. 361-375.

Desai, C. S. and Faruque, M. O. (1983b), "A Generalized Basis for Modelling Plastic Behavior of Materials," Proc., Int. Conf. on Const. Laws for Eng. Mat., Theory and Application, University of Arizona, Tucson, AZ, pp. 201-202.

Desai, C. S., Siriwardane, H. J. and Janardhanam, R. (1982), "Interaction and Load Transfer Through Track Support System, Part 1 & 2, Report DOT-OS-80013, Univ. of Arizona.

Desai, C. S. and Siriwardane, H. J. (1974), "Constitutive Laws for Engineering Materials," Prentice-Hall, Inc., Englewood Cliffs, N. J., p. 468.

Drucker, D. C. and Prager, W. (1952), "Soil Mechanics and Plastic Analysis of Limit Design," Quart. Appl. Math., Vol. 10, No. 2, pp. 157-165.

Drucker, D. C. (1951), "A More Fundamental Approach to Plastic Stress-Strain Relations," Proceedings, 1st U.S. National Congress on Applied Mechanics, pp. 487-491.

Faruque, M. O. (1980), "Development of a Generalized Constitutive Model and Its Implementation in Soil-Structure Interaction," Ph. D. Dissertation, University of Arizona, Tucson, AZ, U.S.A.

Hannant, D. J. (1974), "Nomograms for the failure of Plain Concrete Subjected to Short-Term Multiaxial Stresses," The Structural Engineer. Vol. 52, No. 5, pp. 151-165.

Janardhanam, R. (1980), "Constitutive Laws of Materials in Track Support Structures," Ph.D. Dissertation, Virginia Tech, Blacksburg.

Lade, P. V. (1982), "Three-Parameter Failure Criterion for Concrete," Journal of the Engineering Mechanics Division, ASCE, Vol. 108, No. EM5, Proc. Paper 17383.

Mitchell, J. K. (1976), "The Properties of Cement-Stabilized Soils," Proc. Work Shop on Materials and Methods for Low Cost Road, Rail and Reclamation Works, Leura, Australia, pp. 365-404.

Munster, C. L. (1981), "Constitutive Modelling of Granular Soil Under Three-Dimensional States of Stress," M.S. Thesis, Virginia Tech, Blacksburg.

Salami, M. R. (1986), "Constitutive Modelling of Concrete and Rocks Under Multiaxial Compressive Loading," Doctoral Dissertation, Department of Civil Engineering and Engineering Mechanics, University of Arizona, Tucson, Arizona, U.S.A.

Salami, M. R. and Desai, C. S. (1987), "A Constitutive Model for Plain Concrete," Proceeding of the Second International Conference on Constitutive Laws for Engineering Materials: Theory and Application, Volume I, Tucson, AZ, U.S.A., January 5-8, pp. 447-455.

Task Committee (1982), "Finite Element Analysis of Reinforced Concrete," Chapter 2 in Committee on Concrete and Masonry Structures," Structural Division, ASCE, New York, NY , pp. 34-137.

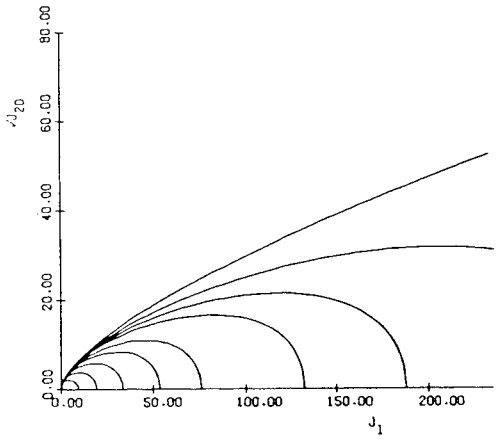

Fig. 1 - Predicted ultimate envelopes in $\sqrt{J_{2D}} - J_1$.

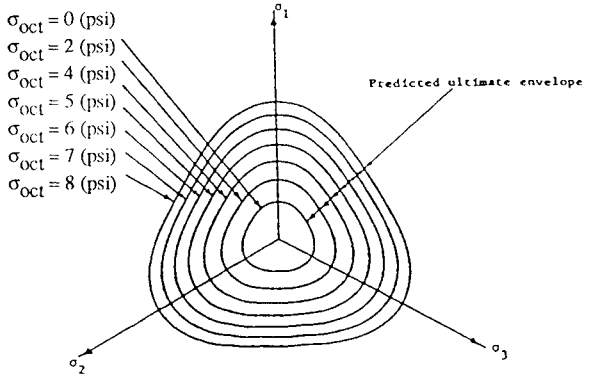

Fig. 2 - Predicted ultimate envelopes in octahedral planes for silty sand. (1.0 psi = 6.89 kPa)

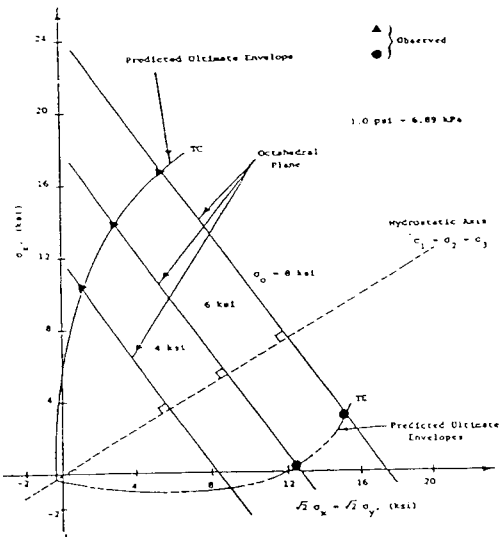

Fig. 3 - Ultimate date and predicted ultimate envelopes in triaxial (1.0 psi = 6.89 kPa)

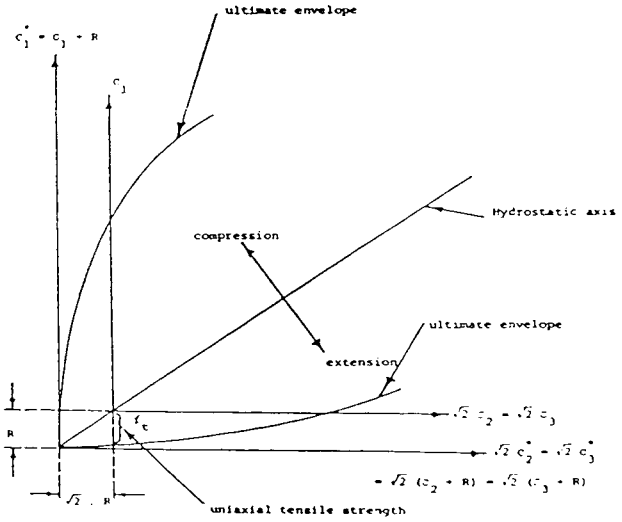

Fig. 4 - Translation of principal stress space along hydrostatic axis to include effect of tensile strength in ultimate criterion for cohesive soils.

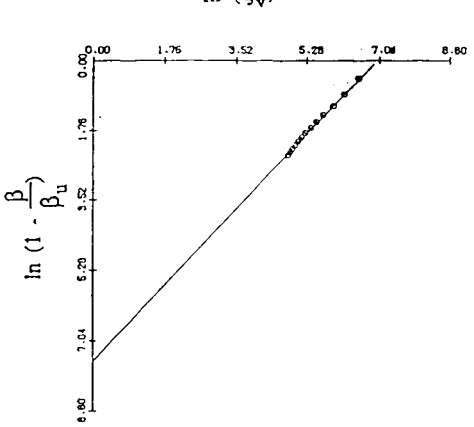

Fig. 5 - Plot of ln (1 - $\frac{\beta}{\beta_u}$) versus - ln (ξ_v) for hydrostatic compression (HC) test for silty soil.

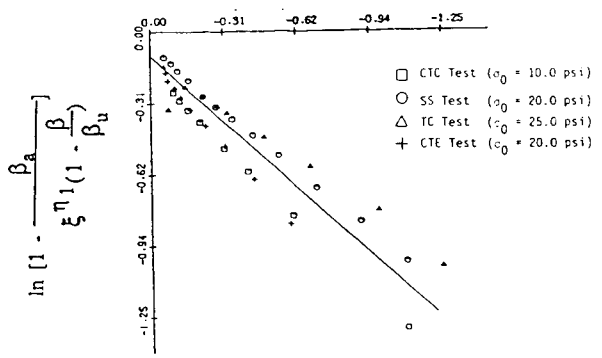

Fig. 6 - Plot of ln [1 - $\frac{\beta_a}{\xi^{\eta_1}(1 - \frac{\beta}{\beta_u})}$] versus - ln ($r_D$) for silty soil

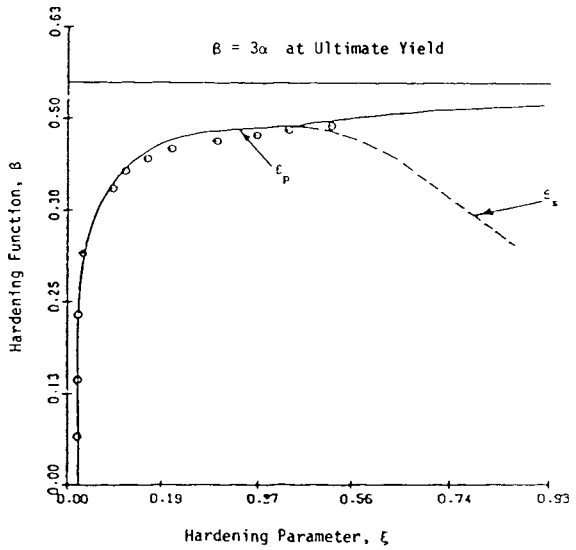

Fig. 8 - Variation of hardening function, β, with respect to the hardening parameter, ξ.

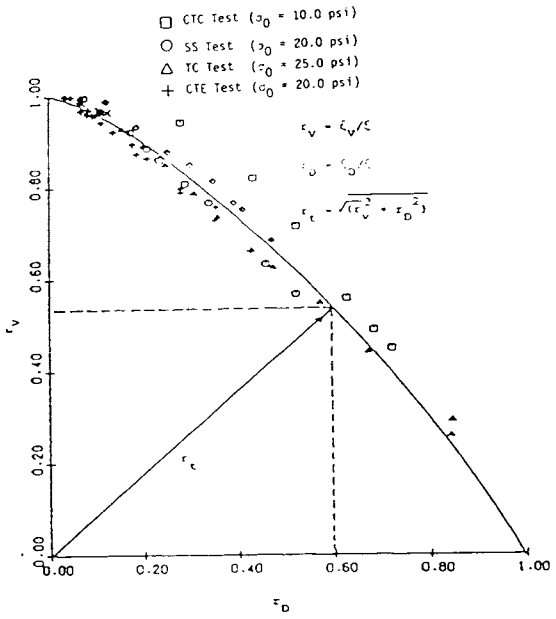

Fig. 7 - r_V versus r_D plot obtained from a number of triaxial tests for silty soil.

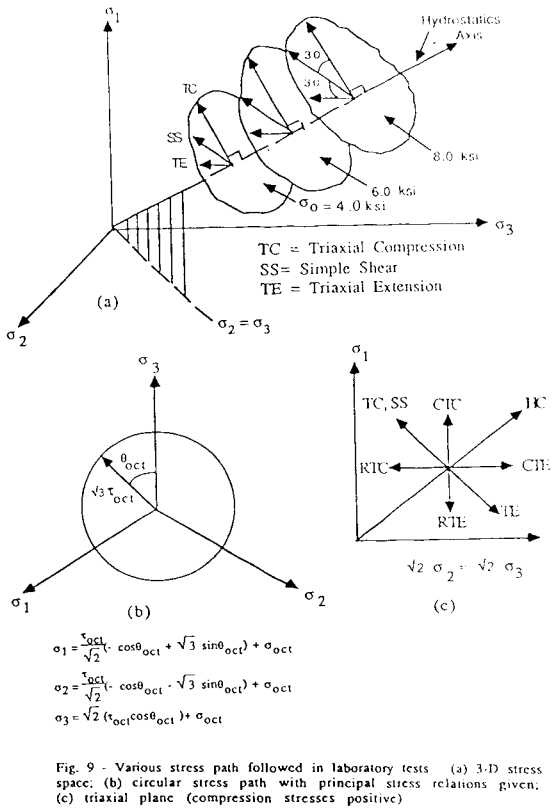

$\sigma_1 = \frac{\tau_{oct}}{\sqrt{2}}(-\cos\theta_{oct} + \sqrt{3}\sin\theta_{oct}) + \sigma_{oct}$

$\sigma_2 = \frac{\tau_{oct}}{\sqrt{2}}(-\cos\theta_{oct} - \sqrt{3}\sin\theta_{oct}) + \sigma_{oct}$

$\sigma_3 = \sqrt{2}(\tau_{oct}\cos\theta_{oct}) + \sigma_{oct}$

Fig. 9 - Various stress path followed in laboratory tests (a) 3-D stress space; (b) circular stress path with principal stress relations given; (c) triaxial plane (compression stresses positive)

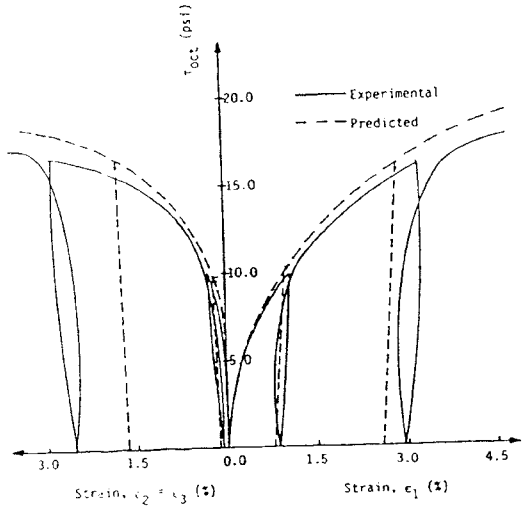

Fig. 10 - Stress versus strain response curve for convensional triaxial compression (CTC) test (σ_o = 10.0 psi) for silty soil. (1.0 psi = 6.89 kPa)

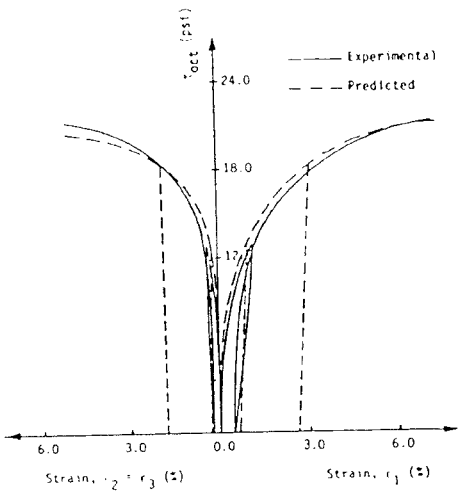

Fig. 12 - Stress versus strain response curve for triaxial compression (TC) test (σ_o = 10.0 psi) for silty soil. (1.0 psi = 6.89 kPa)

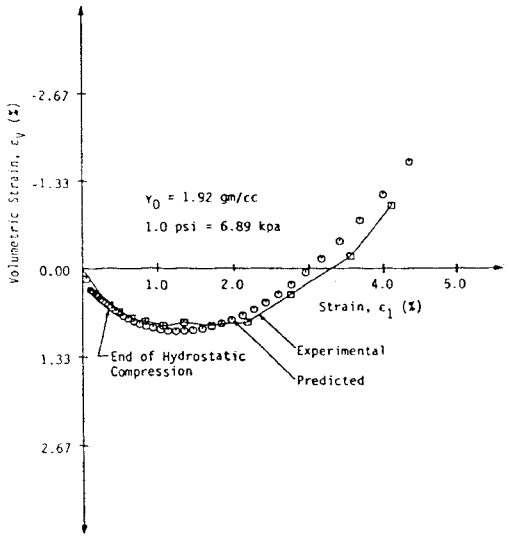

Fig. 11 - Plot of ε_1 versus ε_V of convensional triaxial compression (CTC) test (σ_o = 10.0 psi) for silty soil. (1.0 psi = 6.89 kPa)

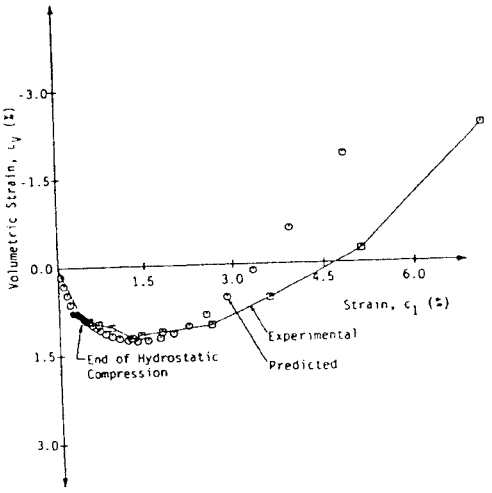

Fig. 13 - Plot of ε_1 versus ε_V of triaxial compression (TC) test (σ_o = 10.0 psi) for silty soil. (1.0 psi = 6.89 kPa

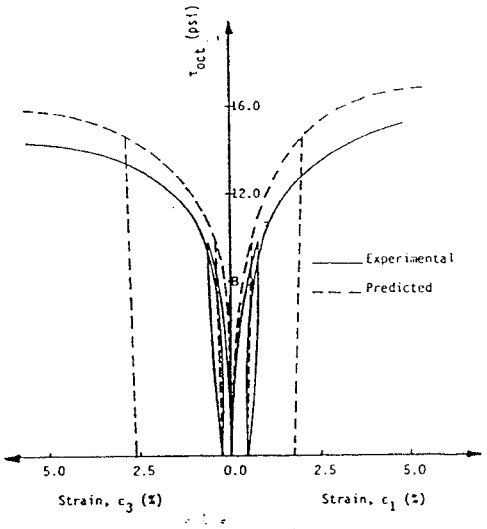

Fig. 14 - Stress versus strain response curve for simple shear (SS) test (σ_o = 20.0 psi) for silty soil. (1.0 psi = 6.89 kPa)

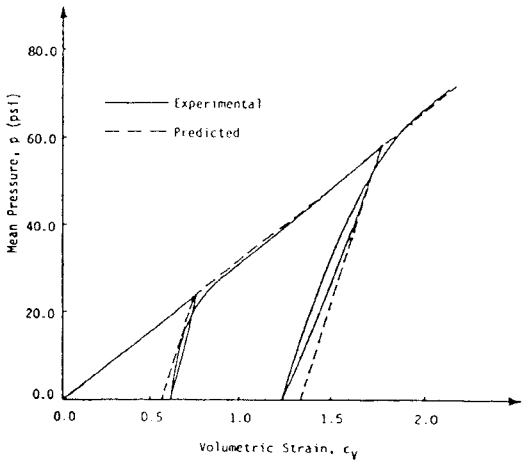

Fig. 16 - Average stress versus strain response for hydrostatic compression (HC) test for silty soil.

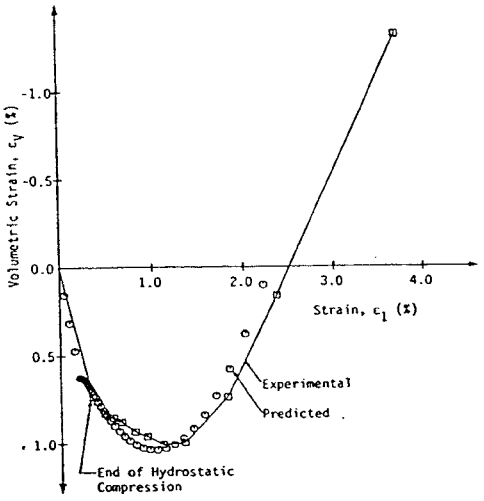

Fig. 15 - Plot of ε_1 versus ε_V of simple shear (SS) test (σ_o = 20.0 psi) for silty soil. (1.0 psi = 6.89 kPa)

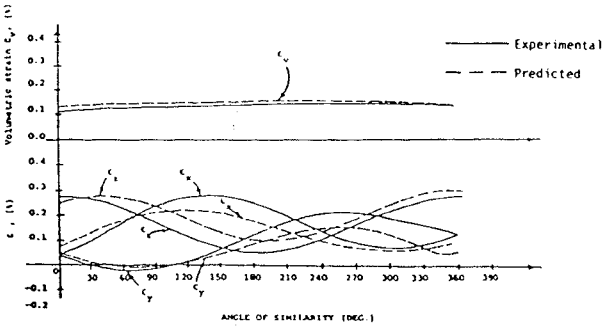

Fig. 17 - Circular stress path. (CPS)